A Southern Sky and Galactic Plane Survey for Bright Kuiper Belt Objects

Scott S. Sheppard[1], Andrzej Udalski[2], Chadwick Trujillo[3], Marcin Kubiak[2], Grzegorz Pietrzynski[2], Radoslaw Poleski[2], Igor Soszynski[2], Michal K. Szymański[2], and Krzysztof Ulaczyk[2]

ABSTRACT

About 2500 square degrees of sky south of declination -25 degrees and/or near the galactic plane were surveyed for bright outer solar system objects. This survey is one of the first large scale southern sky and galactic plane surveys to detect dwarf planets and other bright Kuiper Belt objects in the trans-Neptunian region. The survey was able to obtain a limiting R-band magnitude of 21.6. In all, 18 outer solar system objects were detected, including Pluto which was detected near the galactic center using optimal image subtraction techniques to remove the high stellar density background. Fourteen of the detections were previously unknown trans-Neptunian objects, demonstrating that the southern sky had not been well-searched to date for bright outer solar system objects. Assuming moderate albedos, several of the new discoveries from this survey could be in hydrostatic equilibrium and thus be considered dwarf planets. Combining this survey with previous surveys from the northern hemisphere suggests that the Kuiper Belt is nearly complete to around 21st magnitude in the R-band. All the main dynamical classes in the Kuiper Belt are occupied by at least one dwarf planet sized object. The 3:2 Neptune resonance, which is the innermost well-populated Neptune resonance, has several large objects while the main outer Neptune resonances such as the 5:3, 7:4, 2:1, and 5:2 do not appear have any large objects. This indicates that the outer resonances are either significantly depleted in objects relative to the 3:2 resonance or have a significantly different assortment of objects than the 3:2 resonance. For the largest objects ($H < 4.5$ mag), the scattered disk population appears to have a few times more objects than the main Kuiper Belt population, while the Sedna population could be several times more than that of the main Kuiper Belt.

[1]Department of Terrestrial Magnetism, Carnegie Institution of Washington, 5241 Broad Branch Rd. NW, Washington, DC 20015, USA, sheppard@dtm.ciw.edu

[2]Warsaw University Observatory, Al. Ujazdowskie 4, 00-478 Warszawa, Poland

[3]Gemini Observatory, 670 North A'ohoku Place, Hilo, HI 96720, USA

Subject headings: Kuiper Belt – Oort Cloud – comets: general – minor planets, asteroids – solar system: general – planetary formation

1. Introduction

The strong dynamical connection that the trans-Neptunian objects (TNOs) have to the planets makes determining their population and orbital structures valuable for gaining insight into solar system formation and planet evolution. The Kuiper Belt, a remnant of the original protoplanetary disk, has a "fossilized" record of the original solar nebula and subsequent evolution of the solar system. TNOs are likely primitive with significant amounts of volatiles. The largest TNOs or dwarf planet sized objects are rare but extremely important for several reasons: 1) The brightest few objects are the only ones accessible to high signal to noise spectroscopy techniques that are required to determine surface compositions, such as methane and water ice (Barucci et al. 2008; Trujillo et al. 2011). These physical characteristics are important in order to understand the formation, origin and composition of the objects and gain insight into planet formation and chemistry in the original solar nebula. 2) The size distribution of the biggest objects in the Kuiper Belt determines if the mass in the Kuiper Belt is dominated by the largest or smallest objects, which is a key metric of planetismal growth scenarios (Kenyon et al. 2008, 2010; Cuzzi et al. 2010). The size and number of the biggest objects constrain the density and thus planet formation ability of the original solar nebula in the outer solar system. 3) Occultations of stars by the biggest TNOs are possible to predict and observe in order to probe the TNOs sizes, shapes, albedos, and atmospheres (Elliot and Kern 2003; Elliot et al. 2010).

The Palomar 48 inch Schmidt telescope in the northern hemisphere, with one of the largest CCD cameras in the world, was used to survey most of the sky north of -25 degrees declination for the brightest ($m_R \lesssim 21$ mags) TNOs (Trujillo and Brown 2003; Brown et al. 2004, 2005; Brown 2008; Schwamb et al. 2009, 2010). In these surveys tens of bright TNOs including likely dwarf planets Eris, Makemake, Haumea, Orcus, Quaoar, Sedna and 2007 OR10 were discovered. These surveys showed that many of the largest Kuiper Belt Objects (KBOs) have relatively large inclinations with the vast majority of KBOs expected to be found within about 20 degrees of the ecliptic (Brown 2008). Extrapolating the Cumulative Luminosity Function (CLF) to the bright end of the KBOs indicates several large KBOs should be discovered in the southernmost parts of the sky that the surveys from the northern telescopes did not image.

The southern hemisphere has not been well-surveyed for distant solar system objects until now because in the past there were no sensitive, wide-field digital imagers on suitable

telescopes in the south. This changed in 2009 when a large wide-field imager was put onto the 1.3 meter Warsaw telescope at Las Campanas in Chile. The OGLE-Carnegie Kuiper Belt Survey (OCKS) was implemented to search the Kuiper Belt for dwarf planets and bright TNOs through a shallow survey to fainter than 21st magnitude in the R-band from the southern hemisphere. OCKS covered the area within a few tens of degrees of the ecliptic for declinations less than -25 degrees and the crowded galactic plane fields in the north and south. Another independent southern sky survey for KBOs was started in late 2009 with the Schmidt telescope at La Silla (Rabinowitz 2010). This is the first time most of this sky area was searched for outer solar system objects with modern digital CCD detectors.

2. Observations

The vast majority of the survey fields were obtained with the Warsaw 1.3 meter telescope at Las Campanas observatory in Chile. The telescope is also known as the OGLE telescope (Optical Gravitational Lensing Experiment; Udalski et al. 1994) and OCKS is considered part of the OGLE-IV project. OGLE-IV commenced with the successful commissioning of the new wide-field 1.4 square degree imager at the beginning of 2010. The southern sky Kuiper Belt survey observations at the Warsaw telescope occurred between March and September 2010 while the northern galactic plane fields near the ecliptic were imaged in December 2010 and January 2011. The 1.4 square degree imager has 32 E2V44-82 2048×4102 CCD chips with $0.''26$/pixel. There are four rows and 9 columns of chips. Gaps are generally only a few arcseconds between chips except between the first and second rows and third and fourth rows the gaps are a bit wider at several tens of arcseconds. Readout time for the detector is about 20 seconds.

All fields were within about 2.5 hours of opposition with most being within 1.5 hours. At these opposition distances, the apparent motion of an outer solar system object is dominated by the parallax from the Earth's movement, making confusion of outer solar system objects with foreground main belt asteroids minimal (Luu and Jewitt 1988). Las Campanas is a very dark site with excellent seeing conditions (Thomas-Osip et al. 2011). Most images were obtained with the seeing around 1 arcsecond or less. If the seeing was much worse than 1 arcsecond or if the conditions were not photometric on a given night, observations were not taken. Integrations were 180 seconds with the telescope tracking at sidereal rates. Since there was no preferred VR or R-band filter for the 1.4 square degree imager, a V-band filter was used at the start of the survey for fields West of the Galactic plane. Because of the better seeing conditions in the I-band, the I-band filter was used for fields in the Galactic plane as well as fields East of the Galactic plane. It was found that the V-band and I-band

images obtained similar depths but the I-band was preferred since it was less sensitive to moderate moon brightness. Image reduction was performed by first bias subtracting and then flat-fielding the images.

In addition to the Warsaw data, about 100 square degrees were surveyed using the CTIO 4 meter Blanco telescope with its MOSAIC II camera that covers about a third of a square degree. These data were obtained in June 2009 and 2010 in order to see how well such a program would work on the 4 meter telescope. Images were only 20 seconds in length and reached magnitudes of about 22 in the R-band. Recovery was mostly done at the Warsaw 1.3 meter telescope but some recovery took place at the CTIO 4 meter and Magellan 6.5 meter.

3. Analysis

In total about 2500 square degrees of sky were surveyed in the southern hemisphere or near the galactic plane (Figure 1). Each survey field had at least two hours between the first and last image of a three image sequence. Outer solar system objects were searched for in the survey fields in two complementary ways. One technique used a computer algorithm specifically designed to detect the apparent motion of trans-Neptunian objects (Trujillo and Jewitt 1998; Sheppard and Trujillo 2010) while a second technique used a differencing algorithm (Udalski et al. 1997,2003; Wozniak 2000) on the three images in order to remove the steady state of background stars to look for moving or transient objects. The differencing algorithm was used on all fields and was the only technique used on fields within 15 degrees of the galactic plane.

Both computer algorithms were calibrated to detect moving objects that appeared in all three images from one night and had a motion consistent with being beyond 10 AU (motion slower than about 10 arcseconds per hour). Because of the fine pixel scale and relatively good seeing, the survey was sensitive to objects moving as slow as 0.5 arcseconds per hour. This apparent motion corresponds to objects out to about 300 AU. Since the survey covers many nights, the data from night to night is not all of the same quality. In order to make the data as consistent as possible over the nights, survey fields were only taken in moderate seeing (~ 1 arcsecond) or better conditions and only when conditions were photometric. If the seeing was significantly worse than about one arcsecond, the survey was not continued for that night.

The limiting magnitude of the survey was determined by placing artificial objects in the fields matched to the point spread function of the images with motions mimicking that

of a TNO (4 to 0.5 arcseconds per hour). A 50% detection efficiency at an R-band limiting magnitude of about 21.6 magnitudes was found for fields with good seeing conditions about 15 degrees or more from the galactic plane (Figure 2). For fields with moderate seeing conditions the R-band limiting magnitude was found to be about 21.2 magnitudes, where the typical color of a moderately red KBO was used to convert the I-band survey fields to the R-band (R-I=0.5 mags) in order to better compare the survey with previous survey depths.

For images near the galactic plane the stellar confusion would limit the detection of moving solar system objects in previous surveys. In this survey the optimal PSF matching image subtraction techniques developed by Alard and Lupton (1998) and Alard (2000) and implemented through the previous OGLE phases were used (Wozniak 2000; Wozniak et al. 2001; Udalski 2003). PSF matching and image subtraction removed the stellar confusion from the galactic plane. Thus, this is the first survey to be sensitive to TNOs near the galactic center where the ecliptic plane crosses the galaxy. To test the moving object algoritm with differenced images, Pluto was observed early in the survey and easily found in the dense galactic plane (Figures 3 and 4). The survey depth near the galactic center was similar to the depth of the fields off the galactic plane, but the survey efficiency of detection was decreased by about 15 percent.

4. Results and Discussion

4.1. Completion Limits of the Kuiper Belt

Eighteen outer solar system objects were detected in this survey. Fourteen of these objects were new discoveries showing that this region of sky had not been well-searched for bright, distant objects in the past (Tables 1 and 2). Combining this southern sky and galactic plane survey with the previous large area northern sky surveys (Trujillo and Brown 2003; Brown 2008; Schwamb et al. 2009, 2010) and a recent large Kuiper Belt survey in the south started by Rabinowitz (2010) makes it likely that the Kuiper Belt is now nearly complete to about 21st magnitude in the R-band. To date, only three areas have not been well searched for bright outer solar system objects: 1) southern fields very distant from the ecliptic (> 20 degrees ecliptic latitude) and thus unlikely to harbor many bright KBOs, 2) a few hundred square degrees in the northern section of the north galactic plane near the ecliptic and 3) a few hundred square degrees in the northern section of the south galactic plane near the ecliptic (Figure 1). There are around 70 known TNOs with apparent magnitudes brighter than 21 in the R-band (see section 4.2), almost all within 20 degrees of the ecliptic. Thus, there is on average one KBO brighter than 21st mag every few hundred square degrees of sky near the ecliptic. This means there is likely to be only one or two KBOs brighter than

21st magnitude in the few remaining areas yet to be searched. Though nearly complete to 21st magnitude now, some objects, especially Centaurs and scattered disk objects, have large eccentricities and thus could become brighter than 21st magnitude in the future as they approach perihelion.

The size of an object at the completeness limit depends on the distance and albedo of the object (Figure 5). The largest few objects, with radii greater than about 500 km, have been found to have very high albedos ($\rho_R \sim 0.6 - 0.8$), while smaller objects appear to have moderate albedos ($\rho_R \sim 0.1 - 0.2$) (Stansberry et al. 2008). The high albedos of the largest objects is likely due to atmospheres and/or surface processes such as cryovolcanism (Licandro et al. 2006; Dumas et al. 2007; Rabinowitz et al. 2007; Sheppard 2007). Assuming a typical albedo of $\rho_R = 0.15$ for the moderate sized KBOs of 21st magnitude, the completeness limit at 30 AU is about 80 km in radius, while at 50 AU it is about 225 km in radius (Figure 6). In absolute magnitude, H, this would be 6.6 and 4.4 magnitudes respectively (Figure 7). It is clear that further Pluto or larger sized objects could remain undetected if beyond a few hundred AU.

4.2. Size Distribution

Figure 8 shows the cumulative number of all known TNOs versus their absolute magnitude, H. Objects with absolute magnitudes $H > 7$ mags appear to have a roll-over in their size distribution because of detection biases. The largest KBOs with $H < 3$ mags do not follow the simple power-law found for the objects with $3 < H < 7$ mags (Brown 2008). The largest KBOs have been found to have preferentially higher albedos, likely because of atmosphere effects and surface activity that keep the surfaces young and bright (Jewitt and Luu 2004; Lykawka and Mukai 2005; Schaller and Brown 2007; Stansberry et al. 2008; Desch et al. 2009). The absolute magnitudes the largest KBOs would have if they had a more typical albedo of 0.15 (Brown and Trujillo 2004; Brown et al. 2006; Stansberry et al. 2008) are shown by squares in Figure 8. The squares in Figure 8 fit a simple power-law for all objects with $H < 7$ magnitudes ($r < 60$ km assuming 0.15 albedo).

The points in a cumulative distribution are heavily correlated with one another, tending to give excess weight to the faint end of the distribution. A differential distribution does not suffer from this problem. Figure 9 shows the differential number of all known TNOs versus their absolute magnitude, where, like in Figure 8, the largest few objects have had their absolute magnitudes adjusted for their abnormally high albedos compared to smaller objects. It is clear there is a turnover around an absolute magnitude of 7 mags ($r \sim 60$ km) showing observational bias beyond this magnitude. The best fit power-law for the differential

points finds $q = 3.0 \pm 0.5$ for $H < 7$ magnitudes, where $n(r)dr \propto r^{-q}dr$ is the differential power-law radius distribution with $n(r)dr$ describing the number of TNOs with radii in the range r to $r+dr$. This is slightly lower than most previous fits ($q \sim 4$) that were more heavily dependent on fainter (smaller) objects (Jewitt et al. 1998; Trujillo et al. 2001; Petit et al. 2008; Fraser et al. 2008; Fuentes and Holman 2008; Fraser and Kavelaars 2009; Fuentes et al. 2009). As the scattered disk and Sedna populations are not close to completion on the large end ($H < 4.5$ mags), including such objects (Eris, 2007 OR10 and Sedna), as done here, likely results in a shallower measured slope. The size distributions of individual dynamical classes are likely more informative (see section 4.2.2). There are no obvious discontinuities at the large end of the KBO size distribution when including all dynamical classes of TNOs (Figures 8 and 9).

4.2.1. Dwarf Planets

A dwarf planet is defined by the International Astronomical Union (IAU) as an object that is in hydrostatic equilibrium and has not cleared the neighborhood around its heliocentric orbit of other similarly sized objects. Though the dwarf planet definition is imprecise, it is clear that Ceres in the main asteroid belt as well as Pluto and Eris in the outer solar system are bonafide dwarf planets. Makemake and Haumea are also likely dwarf planets as are the next largest bodies in the outer solar system such as Sedna, 2007 OR10, Orcus and Quaoar. Though the lower size limit of an object in hydrostatic equilibrium is not well defined, Lineweaver and Norman (2010) suggest it could be as small as 200 km in radius for an icy body in the outer solar system. This would put tens more objects in the outer solar system into the dwarf planet category, including three objects discovered in this survey (Table 1: 2010 EK139, 2010 KZ39 and 2010 FX86). The actual sizes and shapes of these bodies are not well known to date and will depend heavily on their albedos and compositions. Further detailed observations are required to determine the true sizes and shapes of the new discoveries.

With most of the biggest Kuiper Belt objects likely known, it is interesting to compare where the largest ($H \leq 4.5$ mags) objects reside dynamically in the Kuiper Belt (Figure 10). At least one of the largest objects can be found in most of the TNO dynamical populations (Tables 3 and 4). The scattered disk population (Gomes et al. 2008) has Eris and 2007 OR10, while Sedna is in its own dynamical class (Morbidelli and Levison 2004; Gladman and Chan 2006) that resides significantly beyond the Kuiper Belt edge (Trujillo and Brown 2001; Allen et al. 2001). The high inclination classical Kuiper belt (Gomes 2003) has several large objects including Makemake, Haumea, Varuna and (278361) 2007 JJ43. Even the low

inclination classical Kuiper belt population, generally known for its smaller sized objects (Levison and Stern 2001), appears to have Quaoar. Further confirming Quaoar's status as a low inclination Kuiper belt object is Quaoar's ultra-red surface (Jewitt and Luu 2004), which is a characteristic generally associated with the low inclination classical Kuiper Belt (Tegler and Romanishin 2000; Trujillo and Brown 2002; Stern 2002; Doressoundiram et al. 2008; Peixinho et al. 2008).

The actual number of Pluto sized bodies is now known (Table 3). Previous authors have argued that the Kuiper Belt likely lost a substantial amount of its mass through collisional grinding and dynamical interactions with the planets (Kenyon and Luu 1999; Levison et al. 2008; Morbidelli et al. 2008; Stewart and Leinhardt 2009). Observationally, many more objects appear to be required in order to produce the observed angular momentum of the largest KBOs (Jewitt and Sheppard 2002; Rabinowitz et al. 2006) and binaries (Noll et al. 2008). Detailed simulations show that Kuiper Belt formation is possible with only the small number of Pluto sized objects observed (Kenyon and Bromley 2008; Schlichting and Sari 2011). A significant number of Pluto sized objects likely exist in the populations beyond 100 AU such as the Sedna types and Oort cloud objects, which are currently too faint to be efficiently detected to date. It is important to determine if the Pluto sized objects formed in the Kuiper Belt as we see it today or if they originated much closer to the Sun and were later transported to their current orbits.

4.2.2. TNO Population Ratios

On the large size end ($H \lesssim 4.5$ mags), the ratio of the (Plutinos):(Main Kuiper Belt):(Scattered Disk):(Sedna Types) was found to be $(1) : (2.6) : (7 \pm 3) : (75\pm^{+115}_{-55})$, respectively (Table 4). Thus the Sedna population could be the dominant observed small body population for dwarf sized planets (Figure 11). The scattered disk population is likely bigger than the main Kuiper Belt (MKB) population by a factor of a few. The Plutino population is smaller by a factor of a few compared to the main Kuiper Belt. Both the scattered disk and main Kuiper Belt populations on the large end of the size distribution ($H \lesssim 4.5$ mags) are consistent with $q = 3.3 \pm 0.7$ while the Plutino population appears significantly shallower than this with $q = 2.2 \pm 0.5$. The scattered disk population size determined from the largest objects ($H < 4.5$ mags) is consistent with Trujillo et al. (2001) estimated from smaller objects in the scattered disk when using a $q \sim 3.3$ size distribution.

4.2.3. The Main Kuiper Belt

The main Kuiper Belt ($39 < a < 48$ AU) appears to be divided into three distinct dynamical classes (Figure 12). The high inclination and low inclination ("cold") classical classes have been suggested for a decade, with the largest objects preferentially in high inclination orbits (Levison and Stern 2001; Brown 2001). When plotting only the largest few objects ($H < 4.5$ mags), there appears to also be both low eccentricity and higher eccentricity classes (Figure 10). All three of the low inclination objects ($i < 10$ degs) with $H < 4.5$ mags have low eccentricities ($e < 0.05$). The high inclination objects with $H < 4.5$ mags in the main Kuiper Belt appear to have either low eccentricities ($0.03 < e < 0.07$; 6 observed) or significantly higher eccentricities ($0.13 < e < 0.16$; 8 observed). Only one of the twenty main Kuiper Belt objects with $H < 4.5$ mags has an eccentricity between these two ranges (Salacia (120347) 2004 SB60 which has $e = 0.10$) while two others have slightly higher eccentricities (Haumea with $e = 0.20$ and (230965) 2004 XA192 with $e = 0.25$).

The Hartigan and Hartigan (1985) dip test for bimodality shows a strong bimodality in eccentricity when including all main Kuiper Belt objects with $H < 4.5$ mags except for the interesting binary object Salacia (these nineteen objects give a dip statistic of 0.145 which corresponds to a confidence of 0.997 for bimodality, a 3 sigma result). Including Salacia in the dip test gives a less significant result of only 0.990 confidence in bimodality, or slightly less than 3 sigma. Including smaller main Kuiper Belt objects decreases the bimodality significance even further. If real, the low versus higher eccentricity populations of highly inclined large objects could have different origins, such as forming in different regions of the solar system or originally from different scattering events during the migration of the planets.

The largest bodies ($H < 4.5$ mags) are too few for meaningful statistics, but it appears that the high inclination main Kuiper Belt does not have a significantly shallower power-law distribution than the low inclination population, as was found for the smaller objects of these two populations by Fraser et al. (2010) (Figure 12). There is a possible deficiency of objects in the main Kuiper Belt between $2.5 < H < 3.5$ magnitudes, but this is likely not statistically significant as it is just small number statistics.

4.2.4. Resonance Populations

A surprising result is the absence of large objects in all the main Neptune resonance populations except the 3:2 resonance (see Gladman et al. 2008 and Elliot et al. 2005 for resonance calculations as well as the updated version of Elliot et al. 2005 kept by Marc Buie

at www.boulder.swri.edu/buie/kbo/astrom). The Plutinos or 3:2 resonance objects include some of the largest known KBOs such as Pluto, Orcus and Ixion (Table 3) while the other observed heavily populated resonances such as the 5:3, 7:4, 2:1, and 5:2 have no known large KBOs (Table 4). Any object in the Neptune resonances brighter than 21st magnitude ($r \gtrsim 200$ km), would likely have been detected by now (Figure 7 and Table 4). The 5:2 has a few sizable objects with absolute magnitudes of around 3.8 and 5.1 mags, (84522) 2002 TC302 and (26375) 1999 DE9, respectfully. The largest 2:1 object appears to be (119979) 2002 WC19 with an absolute magnitude of 5.1 mags. None of the other resonances have any objects with absolute magnitudes brighter than 5 mags. 2010 EK139, discovered in this survey, appears to be one of the only known objects in the very distant 7:2 resonance (based on orbit calculations from Marc Buie's website at www.boulder.swri.edu/buie/kbo/astrom that has up to date information first published in Elliot et al. 2005).

The relative populations of the various Neptune resonances are currently not well constrained since observational biases make discoveries easier in the closer 3:2 resonance (Jewitt et al. 1998; Trujillo et al. 2001). There is also a strong longitude and latitude dependence on discovery of resonance populations (Chiang and Jordan 2002; Chiang et al. 2003). Previous observational works have suggested that the 2:1 resonance appears to have less objects than the 3:2 resonance (Jewitt et al. 1998; Chiang and Jordan 2002). Numerical simulations of resonance sweeping (Hahn and Malhotra 2005) have shown that the main Neptune resonance populations relative to the 3:2 resonance population may be 2:1 (x2), 7:4 (x0.8), 5:3 (x0.6), 5:2 (x0.5). These simulations suggest that the outer resonances should have a factor of four more objects than the 3:2 resonance. Thus, if 3 very large objects such as Pluto, Orcus and Ixion were found in the 3:2 resonance population, based on Poisson statistics, one would expect 12 ± 3.5 objects of similar size in the other resonances. This is not the case, and such a scenario can be rejected with 3.5 sigma confidence, so either the outer resonances are significantly less populated than the 3:2 resonance or the outer resonance bodies have a different size distribution than the 3:2 resonance. It is likely that the 3:2 resonance is populated by objects that formed significantly closer to the Sun than the outer resonances. Objects forming closer to the Sun would likely accrete more material in a shorter amount of time allowing them to become larger before they were captured in the Neptune resonances. With the Kuiper Belt nearly complete to 21st magnitude, it is unlikely that a planet larger than Mercury within a few 100 AU currently exists. Lykawka and Mukai (2008) suggested such a planet could have disrupted the outer resonance populations. It is still possible that a close stellar encounter or now defunct outer planet could have disrupted or depleted the outer resonances early in the solar system's history.

5. Summary

The OGLE Carnegie Kuiper belt Survey (OCKS) is one of the first southern sky and galactic plane surveys for bright outer solar system objects. Eighteen bright Trans-Neptunian objects were discovered, including some of the most southern outer solar system objects ever detected as well as the intrinsically brightest solar system objects discovered in several years (2010 EK139 with $H = 3.8$ and 2010 KZ39 with $H = 3.9$ mags).

1) A total of 2500 square degrees was searched in the survey. About 2200 square degrees of the survey was south of declination -25 degrees, where northern KBO surveys cannot efficiently observe. The surveyed area includes almost all of the southern sky within about 20 degrees of the ecliptic. Another 300 square degrees of sky was surveyed in the northern galactic plane near the ecliptic using optimal image subtraction techniques to remove the stellar background.

2) The survey obtained a limiting R-band magnitude of 21.6 during optimal observing conditions using the 1.3 meter Warsaw telescope at Las Campanas observatory in Chile. In moderate seeing the survey limit was 21.2 magnitudes in the R-band. During bad seeing conditions the survey was not performed.

3) Kuiper Belt surveys are now nearly complete to about 21st magnitude in the R-band. The corresponding size of an object at 21st magnitude depends on the distance and albedo of the object. At 30 AU 21st magnitude corresponds to about $H = 6.6$ mags while at 50 AU $H = 4.4$ mags, which when assuming a moderate albedo of $\rho_R = 0.15$ correspond to radii of 80 km and 225 km respectively. Through looking at the cumulative luminosity function of the Kuiper Belt objects, significant incompleteness in the main Kuiper Belt probably starts around a radius of 100 km ($H \sim 6$ mags) and becomes drastic around a radius of 60 km ($H \sim 7$ mags.).

4) For the largest objects ($H \lesssim 4.5$ mag), the ratio of the population sizes for the various dynamical reservoirs in the outer solar system were found to be $(1) : (2.6) : (7\pm3) : (75\pm^{+115}_{-55})$, for the (Plutinos):(Main Kuiper Belt):(Scattered Disk):(Sedna Types), respectively. Thus the scattered disk population is likely a few times larger than the main Kuiper Belt population and several times larger than the Plutino population. The Sedna type population likely is the biggest of all the observed outer solar system reservoirs but remains largely unknown because of the strong observational bias against finding very distant objects.

5) Beyond the Kuiper Belt edge, at a few hundred AU or so, there could easily be more Pluto, Mercury or even larger sized objects in Sedna-like orbits. No new Sedna-like objects were detected even though the survey was sensitive to objects up to about 300 AU. Sedna is likely one of the larger and thus one of the brighter members of its population. Any

further Sedna-like object detections will likely require significantly fainter magnitudes while still covering large areas of sky. Pan-Starrs has a chance to detect some Sedna like objects since it will survey large areas of sky to around a magnitude fainter than this survey, but LSST will be needed to find significant numbers of Sedna like objects since sensitivity and large areas of sky are needed to probe this distant, faint population.

6) All the major populated dynamical reservoirs in the Kuiper Belt, including the scattered disk, high inclination classical belt, low inclination classical belt (Quaoar), Sedna and the Plutinos are occupied by dwarf planet sized objects. Only the well-populated outer Neptune mean motion resonances such as the 2:1, 7:4, 5:2, and 5:3 are not occupied by a dwarf planet sized object. Any dwarf planet in these outer resonances would likely have been found to date, suggesting the outer resonances are occupied by a different mix of objects than the 3:2 resonance population or are significantly depleted in objects relative to the 3:2 resonance.

7) The scattered disk and main Kuiper Belt were found to have a power-law size distribution of $q = 3.3 \pm 0.7$ for the largest few objects ($H < 4.5$ mags), while the Plutino population has a shallower slope of $q = 2.2 \pm 0.5$. The high and low inclination main Kuiper Belt populations appear to have similar slopes in their size distributions.

8) The main Kuiper Belt could have three distinct dynamical classes: (1) low inclination with low eccentricity ($e < 0.05$), (2) high inclination with low eccentricity ($e < 0.07$), and (3) high inclination with higher eccentricities ($e > 0.13$).

Acknowledgments

REFERENCES

Alard, C. 2000, A&AS, 144, 363.

Alard, C. and Lupton, R. 1998, ApJ, 503, 325.

Allen, L., Bernstein, G. and Malhotra, R. 2001, ApJ, 549, L241.

Barucci, M., Brown, M., Emery, J. and Merlin, F. 2008, in The Solar System Beyond Neptune, ed. M. Barucci, H. Boehnhardt, D. Cruikshank and A. Morbidelli (Tucson: Univ of Arizona Press), 143-160.

Brown, M. 2001, AJ, 121, 2804.

Brown, M. and Trujillo, C. 2004, AJ, 127, 2413.

Brown, M., Trujillo, C. and Rabinowitz, D. 2004, ApJ, 617, 645.

Brown, M., Trujillo, C. and Rabinowitz, D. 2005, ApJ, 635, L97.

Brown, M. Schaller, E., Roe, H., Rabinowitz, D. and Trujillo, C. 2006, ApJ, 643, L61.

Brown, M. 2008, in The Solar System Beyond Neptune, ed. M. Barucci, H. Boehnhardt, D. Cruikshank and A. Morbidelli (Tucson: Univ of Arizona Press), 335-344.

Chiang, E. and Jordan, A. 2002, AJ, 124, 3430.

Chiang, E., Jordan, A., Millis, R. et al. 2003, AJ, 126, 430.

Cuzzi, J., Hogan, R., and Bottke, W. 2010, Icarus, 208, 518.

Desch, S., Cook, J., Doggett, T. and Porter, S. 2009, Icarus, 202, 694.

Doressoundiram, A., Boehnhardt, H., Tegler, S. and Trujillo, C. 2008, in The Solar System Beyond Neptune, ed. M. Barucci, H. Boehnhardt, D. Cruikshank and A. Morbidelli (Tucson: Univ of Arizona Press), 91-104.

Dumas et al. 2007, AA, 471, 331.

Elliot, J. and Kern, S. 2003, EM&P, 92, 375.

Elliot, J., Kern, S., Clancy, K. et al. 2005, AJ, 129, 1117

Elliot et al. 2010, Nature, 465, 897.

Fraser, W. et al. 2008, Icarus, 195, 827.

Fraser, W. & Kavelaars, J. 2009, AJ, 137, 72.

Fraser, W., Brown, M. & Schwamb, M. 2010, 210, 944.

Fuentes, C. & Holman, M. 2008, AJ, 136, 83

Fuentes, C., George, M., & Holman, M. 2009, ApJ, 696, 91

Gladman, B. and Chan, C. 2006, ApJ Lett., 643, L135.

Gladman, B. Marsden, B. and VanLaerhoven, C. 2008, in The Solar System Beyond Neptune, ed. M. Barucci, H. Boehnhardt, D. Cruikshank and A. Morbidelli (Tucson: Univ of Arizona Press), 43-57.

Gomes, R. 2003, Earth Moon Planets, 92, 29.

Gomes, R., Levison, H., Tsiganis, K. and Morbidelli, A. 2005, Nature, 435, 466.

Gomes, R., Fernandez, J., Gallardo, T. and Brunini, A. 2008, in The Solar System Beyond Neptune, ed. M. Barucci, H. Boehnhardt, D. Cruikshank and A. Morbidelli (Tucson: Univ of Arizona Press), 259-273.

Hahn, J. and Malhotra, R. 2005, AJ, 130, 2392.

Hartigan, J. and Hartigan, P. 1985, The Annals of Statstics, 13, 70.

Iorio, L. 2009, MNRAS, 400, 346.

Jewitt, D., Luu, J., Trujillo, C. 1998, AJ, 115, 2125.

Jewitt, D. and Sheppard, S. 2002, AJ, 123, 2110.

Jewitt, D. and Luu, J. 2004, Nature, 432, 731.

Kenyon, S. and Luu, J. 1999, AJ, 118, 1101.

Kenyon, S. and Bromley, B. 2008, ApJ Supplement, 179, 451.

Kenyon, S., Bromely, B., O'Brien, D. and Davis, D. 2008, in The Solar System Beyond Neptune, ed. M. Barucci, H. Boehnhardt, D. Cruikshank and A. Morbidelli (Tucson: Univ of Arizona Press), 293-313.

Kenyon, S and Bromley, B. 2010, ApJ Supplement, 188, 242.

Levison, H. and Stern, S. A. 2001, AJ, 121, 1730.

Levison, H., Morbidelli, A., Vanlaerhoven, C., Gomes, R., and Tsiganis, K. 2008, Icarus, 196, 258.

Licandro, J. et al. 2006, AA, 445, 35.

Lineweaver, C. and Norman, M. 2010, arXiv:1004.1091

Luu, J. and Jewitt, D. 1988, AJ, 95, 1256.

Lykawka, P. S., and Mukai, T. Planetary and Space Science, 53, 1319.

Malhotra, R. 1995, AJ, 110, 420.

Melott, A. and Bambach, R. 2010, MNRAS, 407, L99.

Morbidelli, A.and Levison, H. 2004, AJ, 128, 2564.

Morbidelli, A., Levison, H. and Gomes, R. 2008, in The Solar System Beyond Neptune, ed. M. Barucci, H. Boehnhardt, D. Cruikshank and A. Morbidelli (Tucson: Univ of Arizona Press), 275-292.

Noll, K., Grundy, W., Chiang, E., Margot, J. and Kern, S. 2008, in The Solar System Beyond Neptune, ed. M. Barucci, H. Boehnhardt, D. Cruikshank and A. Morbidelli (Tucson: Univ of Arizona Press), 345-363.

Peixinho, N., Lacerda, P., and Jewitt, D. 2008, AJ, 136, 1837-1845.

Petit, J., Kavelaars, J., Gladman, B. and Loredo, T. 2008, in The Solar System Beyond Neptune, ed. M. Barucci, H. Boehnhardt, D. Cruikshank and A. Morbidelli (Tucson: Univ of Arizona Press), 71-87.

Rabinowitz, D., Barkume, K., Brown, M., Roe, H., Schwartz, M., Tourtellotte, S. and Trujillo, C. 2006, ApJ, 639, 1238.

Rabinowitz, D., Schaefer, B. and Tourtellotte, S. 2007, AJ, 133, 26.

Rabinowitz, D. 2010, Poster presentation at the TNO 2010: Dynamical and Physical Properties of Trans-Neptunian Objects workshop in Philadelphi, PA, USA

Ragozzine, D. and Brown, M. 2007, AJ, 134, 2160.

Schaller, E. and Brown, M. 2007, ApJ, 659, L61.

Schlichting, H. and Sari, R. 2011, ApJ, 728, 68.

Schwamb, M., Brown, M., and Rabinowitz, D. 2009, ApJ, 694, L45.

Schwamb, M., Brown, M., Rabinowitz, D. and Ragozzine, D. 2010, ApJ, 720, 1691.

Sheppard, S. 2007, AJ, 134, 787.

Sheppard, S. and Trujillo, C. 2010, ApJ, 723, 233.

Stansberry, J., Grundy, W., Brown, M., Cruikshank, D., Spencer, J., Trilling, D. and Margot, J. 2008, in The Solar System Beyond Neptune, ed. M. Barucci, H. Boehnhardt, D. Cruikshank and A. Morbidelli (Tucson: Univ of Arizona Press), 161-179.

Stern, S. A. 2002, AJ, 124, 2297.

Stewart, S. and Leinhardt, Z. 2009, ApJ Letters, 691, L133.

Tegler, S. and Romanishin, W. 2000, Nature, 407, 979-981.

Thomas-Osip, J., McCarthy, P., Prieto, G., Phillips, M., and Johns, M. 2011, arxiv:1101.2340

Trujillo, C. and Jewitt, D. 1998, AJ, 115, 1680.

Trujillo, C., Jewitt, D. and Luu, J. 2000, ApJ, 529, L103.

Trujillo, C., Jewitt, D. and Luu, J. 2001, AJ, 122, 457.

Trujillo, C. and Brown, M. 2001, ApJ, 554, L95.

Trujillo, C. and Brown, M. 2002, ApJ, 566, L125.

Trujillo, C. and Brown, M. 2003, EM&P, 92, 99.

Trujillo, C., Sheppard, S. and Schaller, E. 2011, ApJ, 730, 105

Udalski, A., Szymanski, M., Stanek, K. et al. 1994, Acta Astronomica, 44, 165.

Udalski, A., Kubiak, M., and Szymanski, M. 1997, Acta Astronomica, 47, 319.

Udalski, A. 2003, Acta Astronomica, 53, 291.

Wozniak, P. 2000, Acta Astronomica, 50, 421.

Wozniak, P., Udalski, A., Szymanski, M., Kubiak, M., Pietrzynski, G., Soszynski, I. and Zebrun, K. 2001, Acta Astronomica, 51, 175.

Table 1.   New outer Solar System objects discovered in this survey

Name	H (mag)	m_R (mag)	a (AU)	e	i (deg)	R (AU)	r (km)
2010 EK$_{139}$	3.8	19.5	69.1	0.53	29.5	40.5	310[a]
2010 KZ$_{39}$	3.9	20.1	45.8	0.15	26.1	46.3	300[a]
2010 FX$_{86}$	4.3	20.7	47.0	0.08	25.2	46.8	230[a]
2010 EL$_{139}$	5.0	20.1	39.2	0.07	23.0	36.6	190
2010 HE$_{79}$	5.1	19.8	39.3	0.20	15.7	34.9	180
2010 PU$_{75}$	5.3	20.9	43.4	0.08	10.2	40.0	150
2010 JK$_{124}$	5.4	21.2	39.7	0.09	15.6	40.3	140
2009 MF$_{10}$	6.0	21.1	57.5	0.52	26.1	36.1	120
2010 HD$_{112}$	6.5	22.2	44.5	0.03	3.9	43.1	100
2010 JJ$_{124}$	6.6	20.1	83.0	0.72	37.8	24.1	80
2009 MG$_{10}$	7.0	21.7	47.5	0.34	19.9	32.8	70
2010 HG$_{109}$	7.3	21.7	39.8	0.23	29.2	30.5	60
2010 HU$_{113}$	7.4	22.1	36.2	0.03	11.3	35.3	60
2009 ME$_{10}$	7.5	21.0	27.8	0.18	14.7	23.1	50

Note. — Orbital elements are from the Minor Planet Center and are the semimajor axis (a), inclination (i), and eccentricity (e). The radii (r) of the new objects were determined assuming an albedo of 0.15 and using the equation, $r = (2.25 \times 10^{16} R^2 \Delta^2 / p_R \phi(0))^{1/2} 10^{0.2(m_\odot - m_R)}$ where R is the heliocentric distance in AU, Δ is the geocentric distance in AU, $m_\odot$ is the apparent red magnitude of the sun (-27.1), p_R is the red geometric albedo, m_R is the apparent red magnitude of the object and $\phi(0) = 1$ is the phase function at opposition. H is the absolute magnitude of the object.

[a]These objects could be labeled as dwarf planets since their radii are larger than 200 km assuming a moderate or lower albedo.

Table 2.   Known KBOs and Centaurs detected in this survey

Name	H (mag)	m_R (mag)	a (AU)	e	i (deg)	R (AU)	r (km)
(134340) Pluto	-0.7	13.6	39.6	0.25	17.1	31.8	1150
2007 JJ$_{43}$	3.2	19.4	48.0	0.16	12.1	41.7	350
(10199) Chariklo	6.4	17.5	15.8	0.17	23.4	13.8	100
(55576) Amycus	7.8	19.6	25.0	0.39	13.3	16.8	50

Note. — See Table 1 for comments and definitions.

Table 3.   Ten Intrinsically Brightest TNOs

Name	H (mag)	a (AU)	e	i (deg)	Class
(136199) Eris	-1.2	68.0	0.43	43.9	Scattered
(134340) Pluto	-0.7	39.7	0.25	17.1	3:2 Resonance
(136472) Makemake	-0.3	45.4	0.16	29.0	High i Classical
(136108) Haumea	0.2	43.0	0.20	28.2	High i Classical
(90377) Sedna	1.6	510	0.85	11.9	Sedna
(225088) 2007 OR10	1.9	67.3	0.50	30.7	Scattered
(90482) Orcus	2.3	39.2	0.23	20.6	3:2 Resonance
(50000) Quaoar	2.5	43.5	0.04	8.0	Low i Classical
(28978) Ixion	3.2	39.6	0.25	19.6	3:2 Resonance

Note. — The orbital elements are from the Minor Planet Center and are the semimajor axis (a), inclination (i), and eccentricity (e). H is the absolute magnitude and Class is the dynamical classification of the object.

Table 4.   Bright Kuiper Belt Population Statistics

Class	H_{comp} (mag)	r_{comp} (km)	N	Pop Ratio ($N/N_{3:2}$)
3:2	4.5	210	6	1
5:3	4.2	250	0	0/5
7:4	4.1	260	0	0/5
2:1	3.3	380	0	0/3
5:2	2.5	550	0	0/2
Main Kuiper Belt (MKB)	4.1	260	13[a]	13/5[a]
Scattered Disk	4.1[b]	N/A	35 ± 15[b]	$35 \pm 15/5$
Sedna Type	1.6[c]	N/A	75^{+115}_{-55}[c]	$75^{+115}_{-55}/1$
MKB Low i & e	4.6	200	3	3/6
MKB High i, All e	4.1	260	11	11/5
MKB High i & e	4.1	260	8	8/5
MKB High i & Low e	4.6	200	6	6/6

Note. — H_{comp} is the absolute magnitude completion limit for the particular dynamical class while r_{comp} is the radius completion limit assuming an albedo of 0.15. N is the number of objects known within each class with an absolute magnitude equal to or brighter than H_{comp}. The Pop Ratio is the population number ratio of each dynamical class relative to the 3:2 resonance number population at the H_{comp} of that particular dynamical class (i.e. $N/N_{3:2}$).

[a]None of the Haumea family members, except for Haumea itself, are included. The Haumea family members are likely pieces of Haumea and have very high albedos unlike most of the other moderately sized objects with absolute magnitudes around 3 or 4 (see Raggozine et al. 2007; Trujillo et al. 2011).

[b]Since the scattered disk objects spend most of their time near aphelion, which can be up to a few hundred AU, the absolute magnitude completion number here is for objects currently within about 50 AU of the Sun. The total number of possible scattered disk objects with absolute magnitdue brighter than this was determined by taking the number of known objects of this bright-

ness or brighter and a Poisson probability statistic of how many more are currently unobservable in the distant solar system based on the percent of time the known objects would be brighter than 21st magnitude in their orbit.

ᶜike the scattered disk objects, Sedna is only brighter than 21st magnitude near perihelion. Thus for most of Sedna's orbit it would not be detected by the current large area surveys. To account for this, a Poisson probability statistic of how many more Sedna type objects of similar size are unobservable in the distant solar system was determined based on Sedna's orbit.
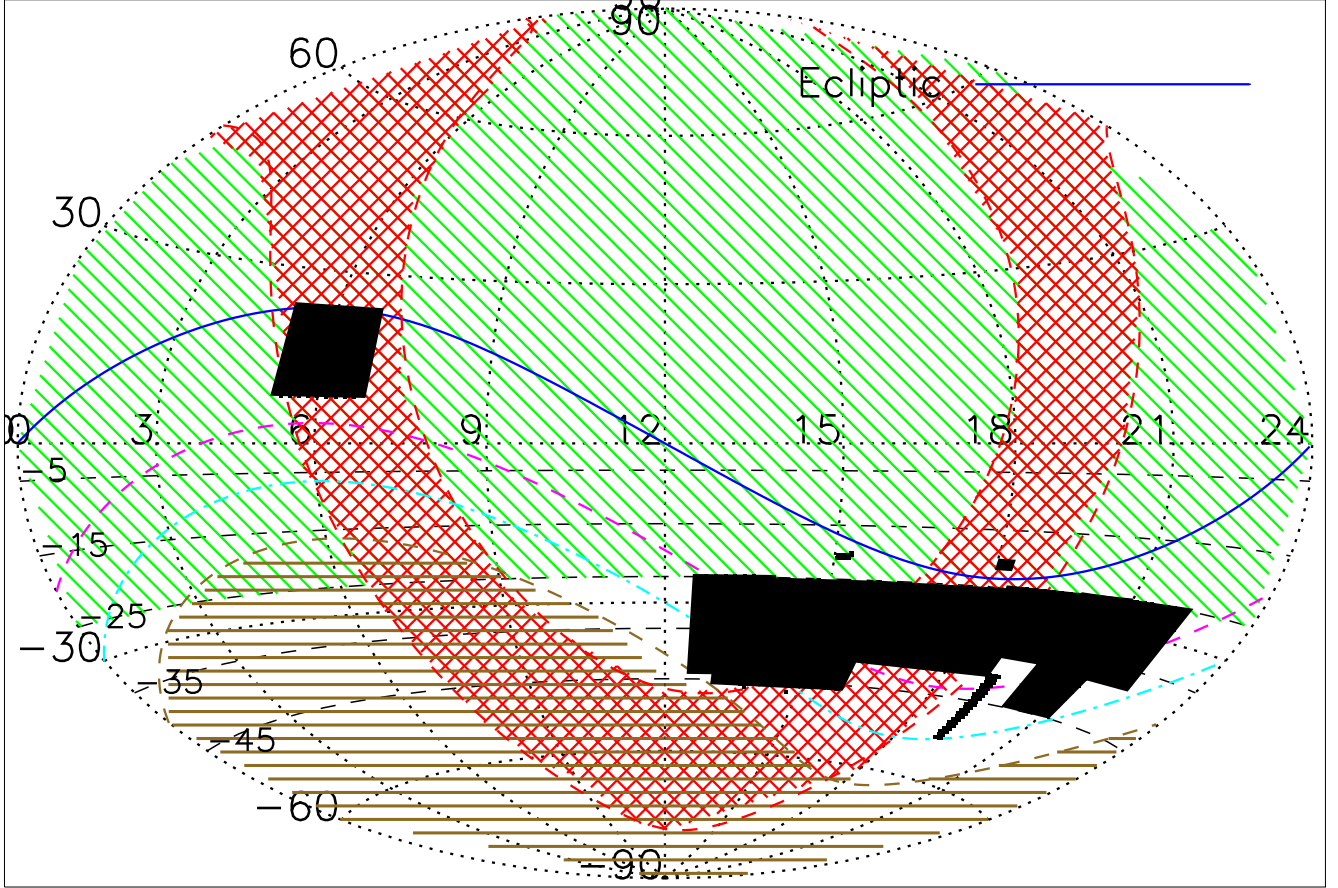
Fig. 1.— The black shaded regions represent the sky area surveyed in this work. The horizontal axis is the right ascension in hours and the vertical axis is the declination in degrees. The blue solid line shows the ecliptic, the purple dashed line shows -20 degrees from the ecliptic and the cyan dotted dashed line shows -30 degrees from the ecliptic. Areas more than -40 degrees south of the ecliptic are shown with brown horizontal stripes. The area within 15 degrees of the galactic plane is shown with red crossed stripes while the area covered by wide-field KBO surveys from the north (Trujillo and Brown 2003; Brown 2008; Schwamb et al. 2009, 2010) are shown with green angled stripes. Almost all KBOs are expected to be within 20 degrees of the ecliptic with it highly unlikely any KBO is beyond 40 degrees from the ecliptic (Brown 2008).
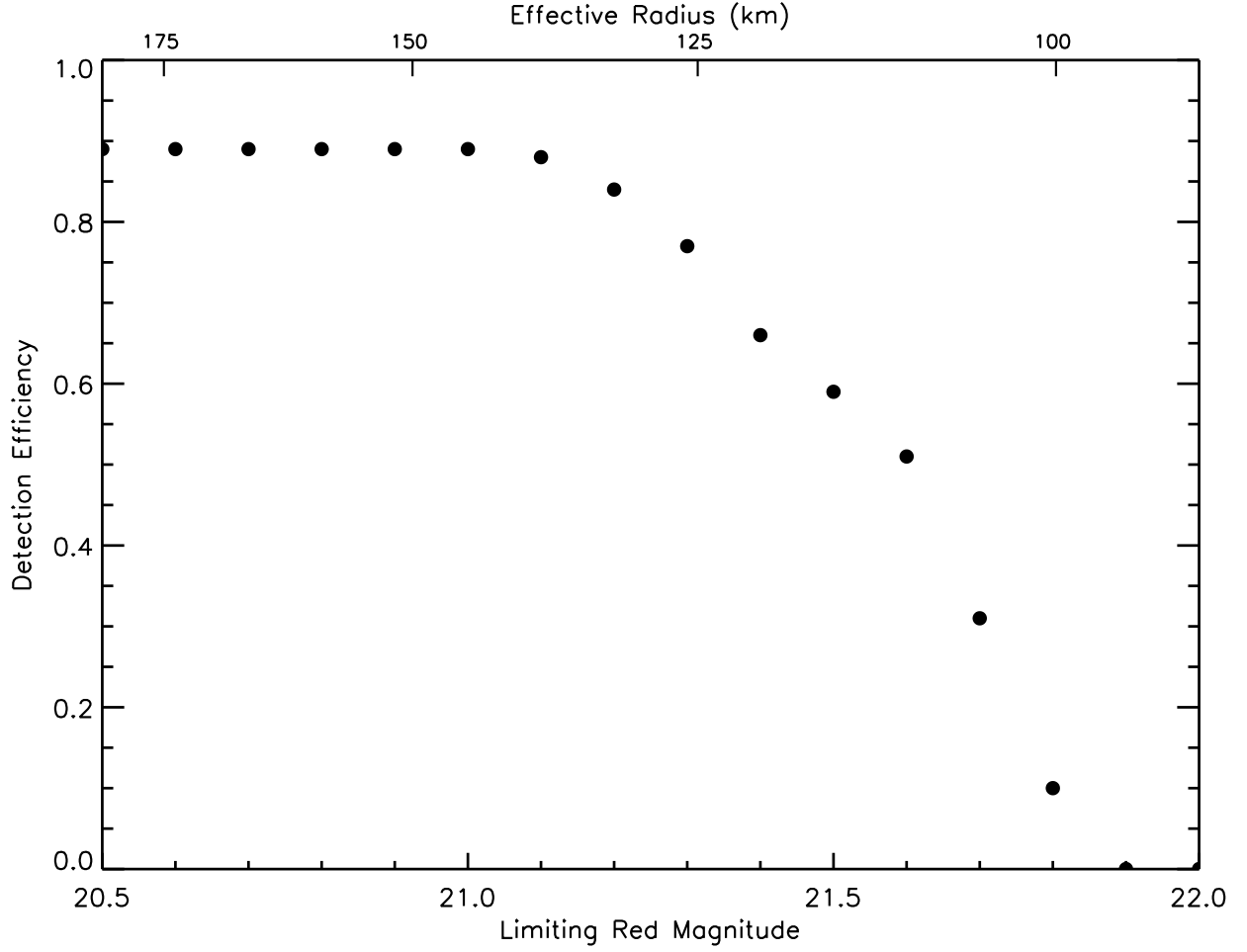
Fig. 2.— Detection efficiency of the KBO survey versus the apparent red magnitude using the Warsaw 1.3 meter telescope. In good seeing (0.8 arcseconds FWHM) the 50% detection efficiency is at about 21.6 mags while in moderate seeing (~ 1 arcsecond) it is about 21.2 mags in the R-band. Effective radii of the apparent magnitudes were calculated assuming the object has an albedo of 0.15 and is at 40 AU.
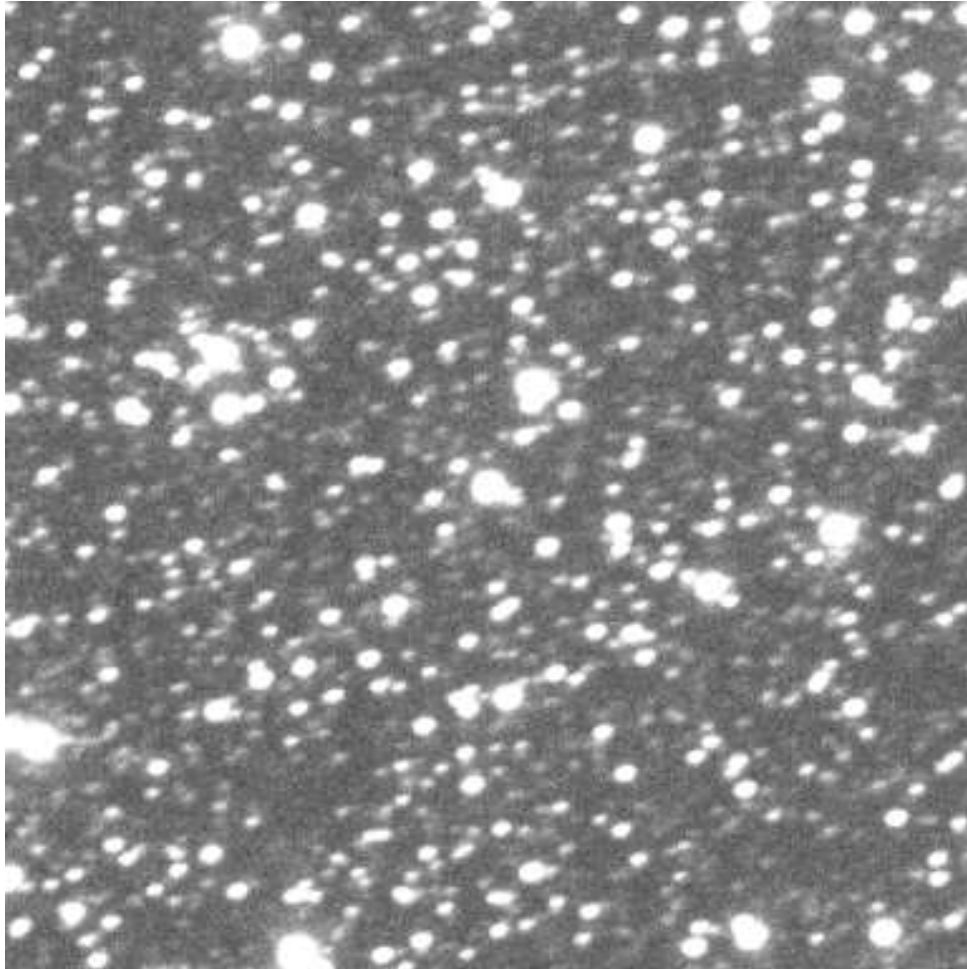
Fig. 3.— A small portion of an image showing Pluto in the galactic plane from the 1.3 meter Warsaw telescope. Pluto is in the center of this image as revealed in Figure 4.

Fig. 4.— A difference image of the Pluto fields (Figure 3) showing the removal of the steady state background of stars. The motion of Pluto is clearly revealed in the difference image as a positive (bright) and negative (dark) point from the subtraction process of the two individual images.
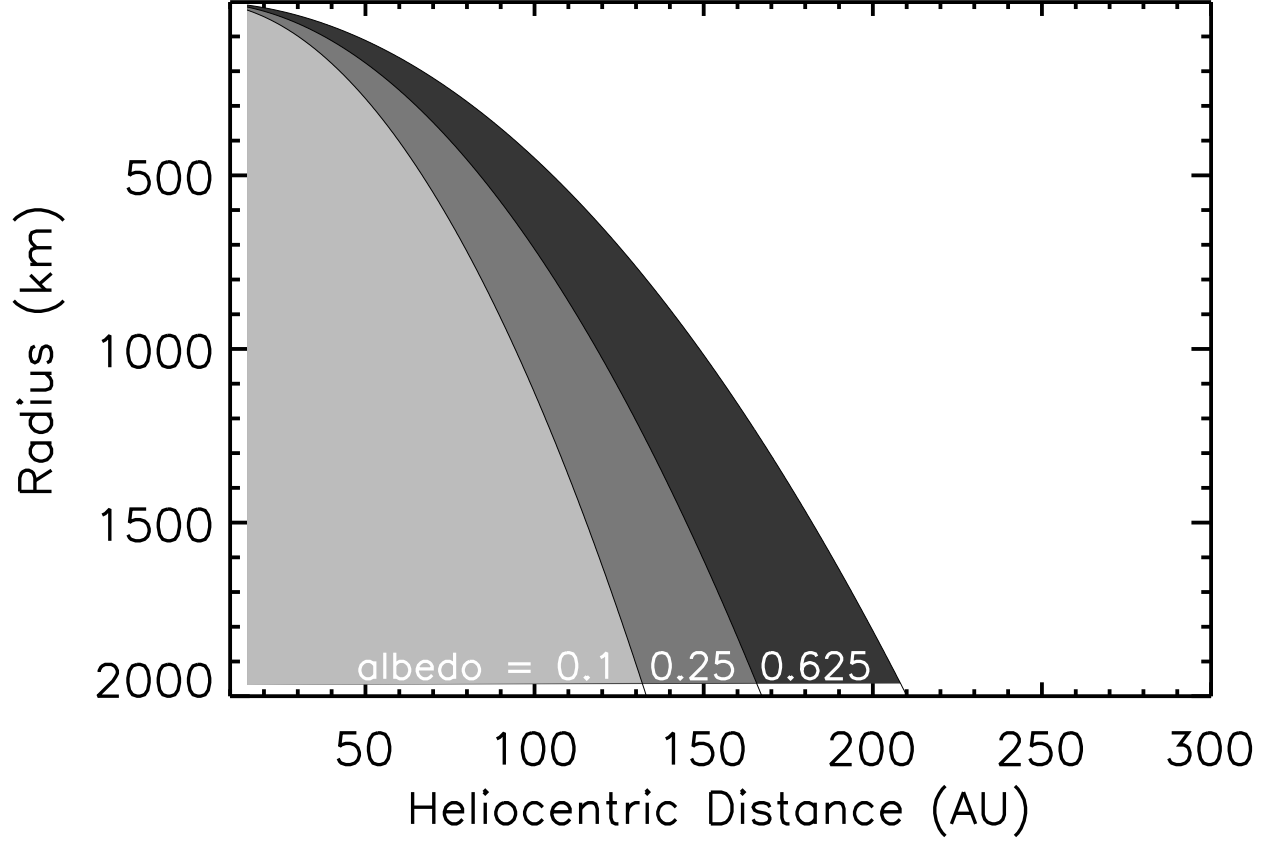
Fig. 5.— The outer solar system has now been surveyed to a completeness limit of about 21 magnitudes in the R-band. This figure shows what size and distance an object would be for several different albedos for a 21st magnitude object. Shaded areas correspond to completeness limits for albedo < 0.1 (light), albedo < 0.25 (medium) and albedo < 0.625 (dark). It is clear that a Pluto (1161 km) or even larger sized object could easily have gone undetected to date if beyond a few hundred.
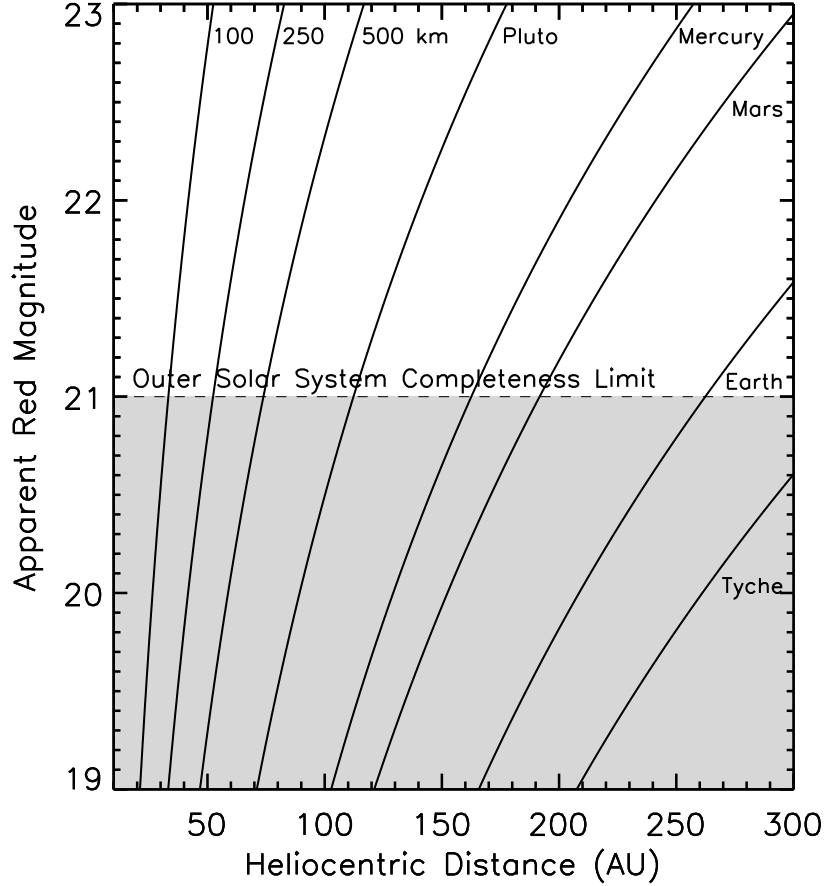
Fig. 6.— The radius of an object is shown assuming a moderate albedo of 0.15 for various heliocentric distances and apparent red magnitudes. The known objects in the Kuiper Belt region are complete to about 21st magnitude, shown by the shaded region below the dashed line. It is likely that everything under the dashed line at 21 magnitudes is known. The radii used for the named objects in the figure are Pluto (1161 km), Mercury (2440 km), Mars (3396 km), Earth (6371 km) and an arbitrary lower limit on a hypothetical eccentric giant planet or companion to our Sun, sometimes called Nemesis or Tyche, with 10,000 km radius (Iorio 2009; Melott and Bambach 2010). In the distant solar system very large objects would easily be undetected to date.
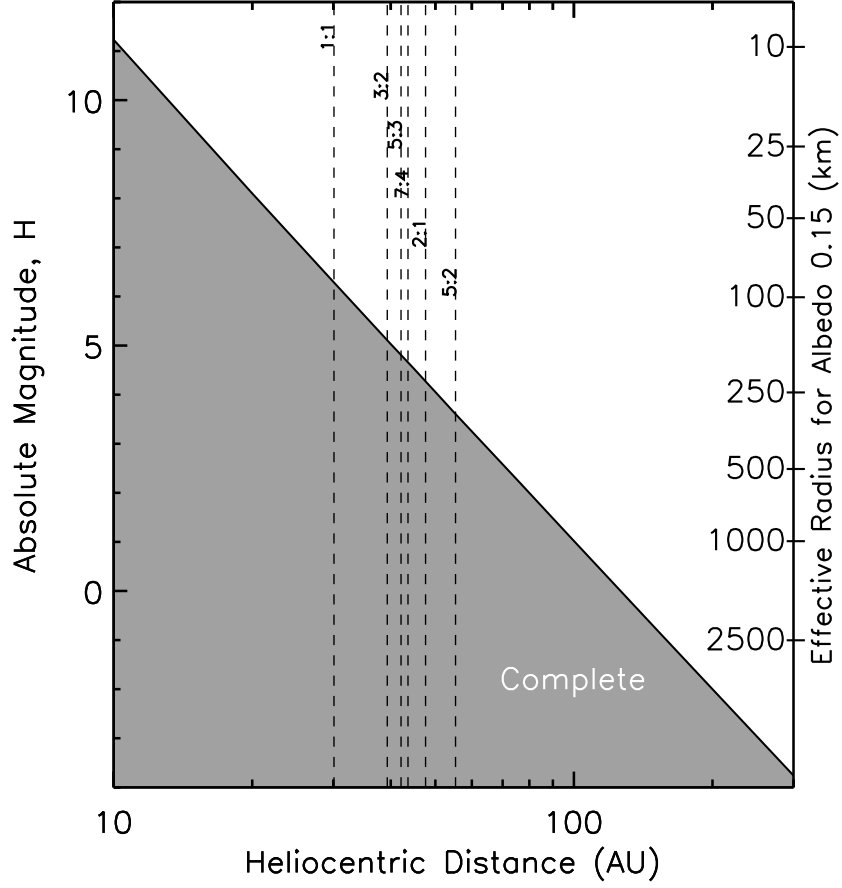
Fig. 7.— The heliocentric distance versus the completeness of absolute magnitude, H. The shaded region shows where the outer solar system should be complete in discoveries. The effective radius on the right side assumes an albedo of 0.15. The average semi-major axis for the various major Neptune resonance populations are shown as vertical dashed lines for reference.
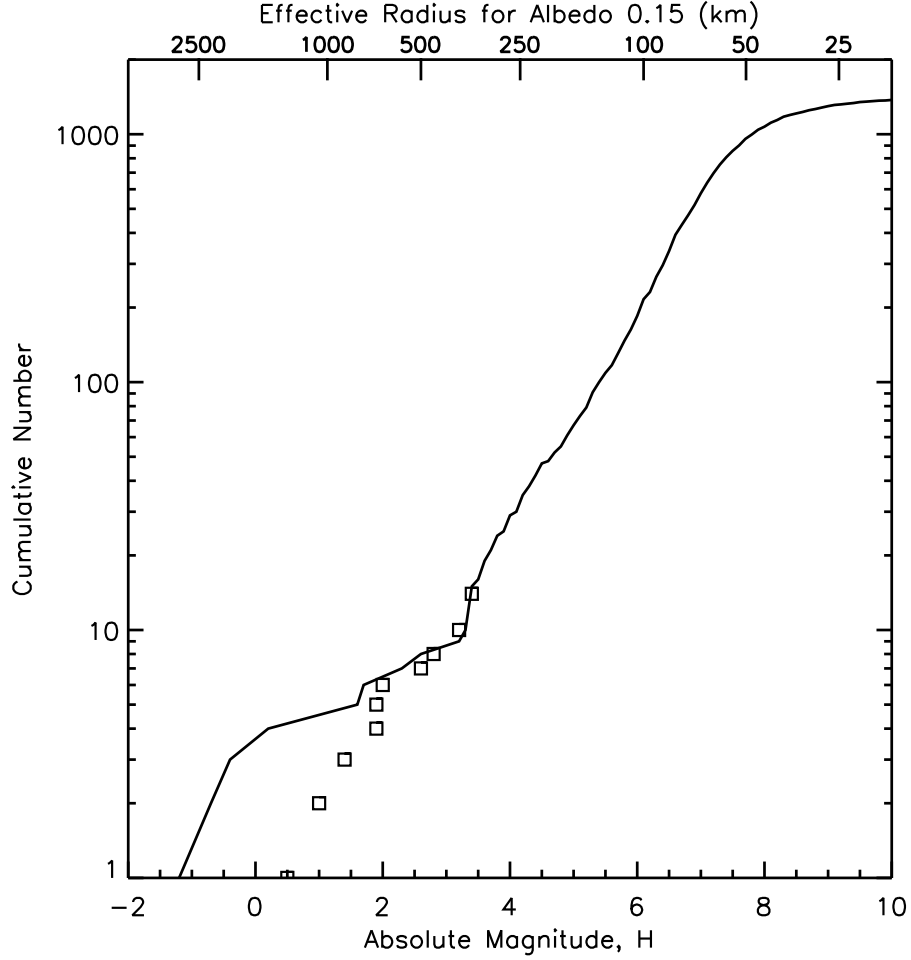
Fig. 8.— The absolute magnitude versus the cumulative number of all known trans-Neptunian objects (solid line). The absolute magnitudes for the largest objects appear overly bright since these objects have much higher albedos than most smaller KBOs. Squares show the absolute magnitudes that the largest KBOs would have if their albedos were 0.15 and not around 0.7 as has been found for Eris, Pluto, Makemake and Haumea. Squares also show the absolute magnitudes the moderately sized KBOs would have if their albedos were not around 0.25 but 0.15 for Sedna, 2007 OR10, Orcus, and Quaoar (Stansberry et al. 2008).
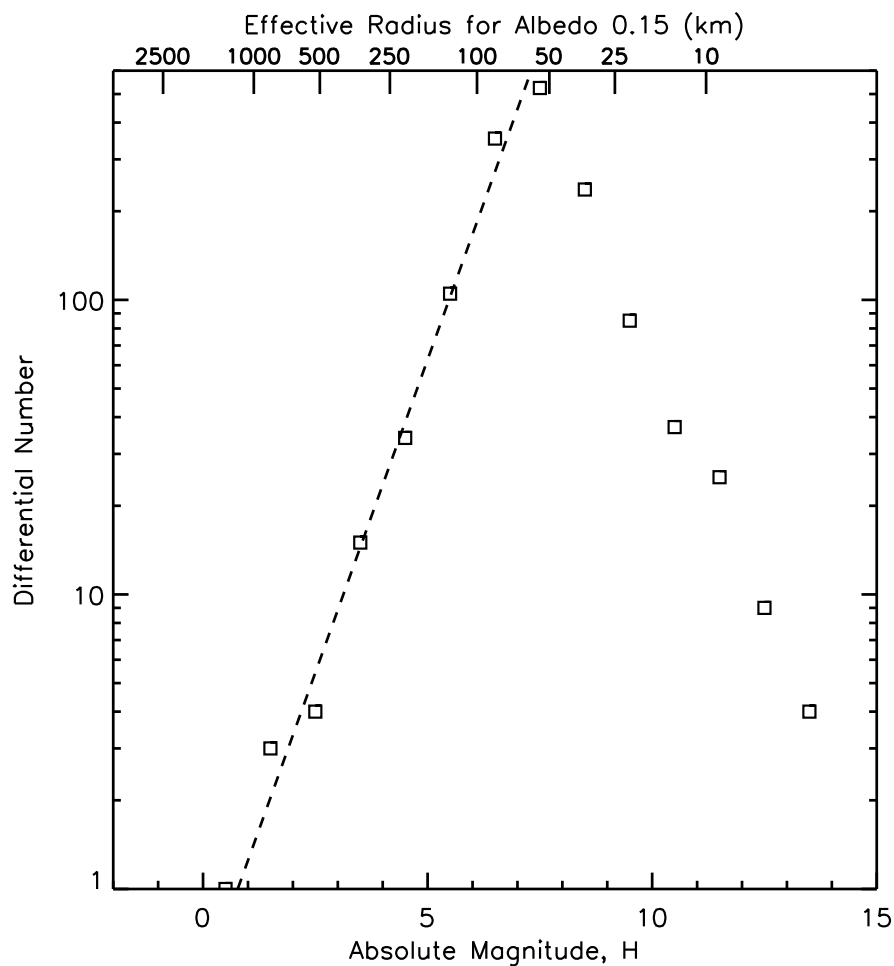
Fig. 9.— The absolute magnitude versus the differential number of known trans-Neptunian objects. Objects are binned in 1 magnitude bins. The largest few objects have had their absolute magnitudes adjusted fainter as in Figure 8 to account for their higher albedos compared to the smaller objects. The dashed line shows the best fit to the largest objects. It is apparent that the Kuiper Belt is nearly complete to about an absolute magnitude of around 5-6 mags after which a turnover shows significant incompleteness.
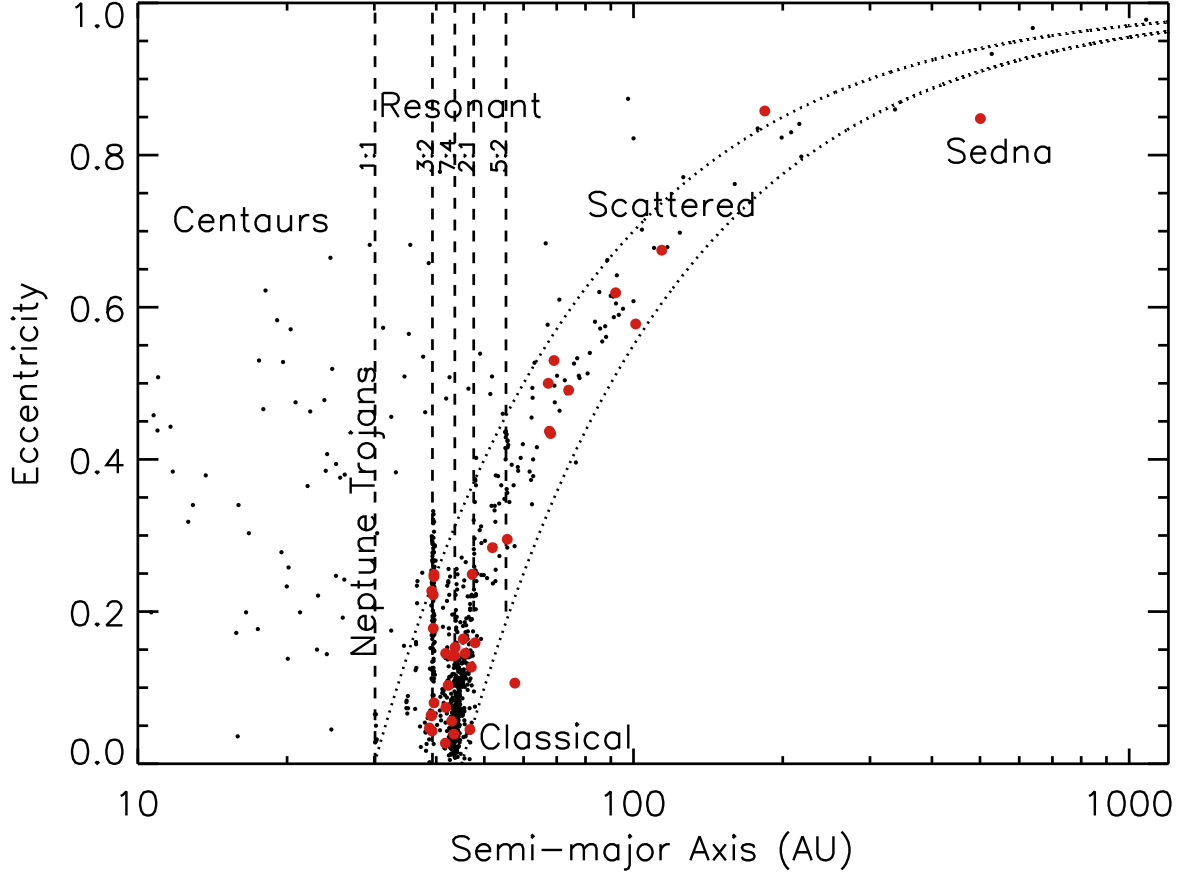
Fig. 10.— The semi-major axis versus eccentricity of multi-opposition trans-Neptunian objects. Large circles represent TNOs with $H \leq 4.5$ mags. This figure shows several distinct dynamical KBO populations. Vertical dashed lines show the main resonances with Neptune as well as the Neptune Trojans in the 1 : 1 resonance. Scattered disk objects have perihelia $30 \lesssim peri \lesssim 45$ AU as shown between the dashed lines. Classical objects are in the lower center portion of the figure and include the the Main Kuiper Belt (MKB) with its high and low inclination populations. There also appears to be a high and low eccentricity population of large objects. An edge near 50 AU can clearly be seen for low eccentricity objects. Centaurs are on unstable orbits between the giant planets. Sedna stands out as being significantly below the perihelion line shown at 40 AU demonstrating its decoupled influence from Neptune unlike the scattered disk objects.
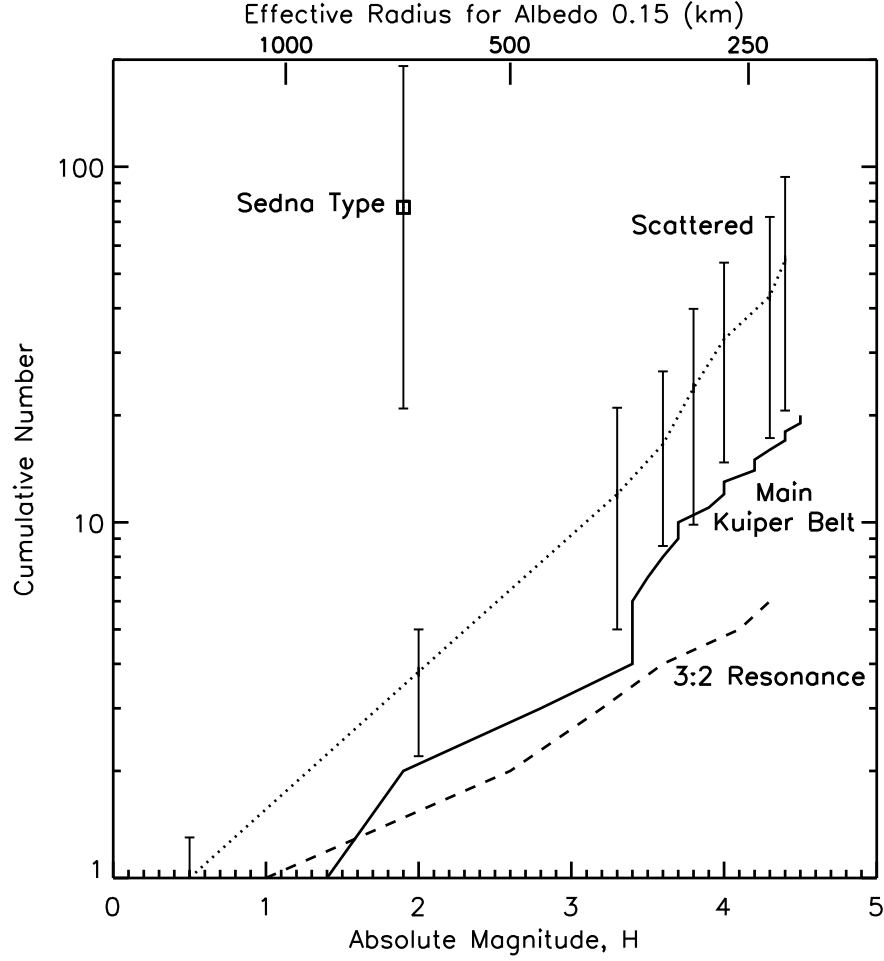
Fig. 11.— The absolute magnitude versus the cumulative number of objects for the various completeness limits (see Table 4) of the dynamical classes in the Kuiper Belt. The largest few objects have had their absolute magnitudes adjusted as in Figure 8 to account for their higher albedos compared to the smaller objects. The Sedna type (square) and scattered disk objects (dotted line) have significant error bars as these populations are not complete for even the largest objects. Poisson statistics were used to extrapolate the total scattered disk and Sedna populations from the known objects brighter than 21st magnitude using the amount of time the objects would be detectable in their eccentric orbits (Table 4). The scattered population is likely larger than either the main Kuiper Belt (solid line) or the 3:2 resonance population (dashed line). The Sedna type population appears to be the largest of all the populations by a factor of ten or more. The 3:2 resonance population has a shallower size distribution slope ($q = 2.2 \pm 0.5$) than the other populations ($q = 3.3 \pm 0.7$).
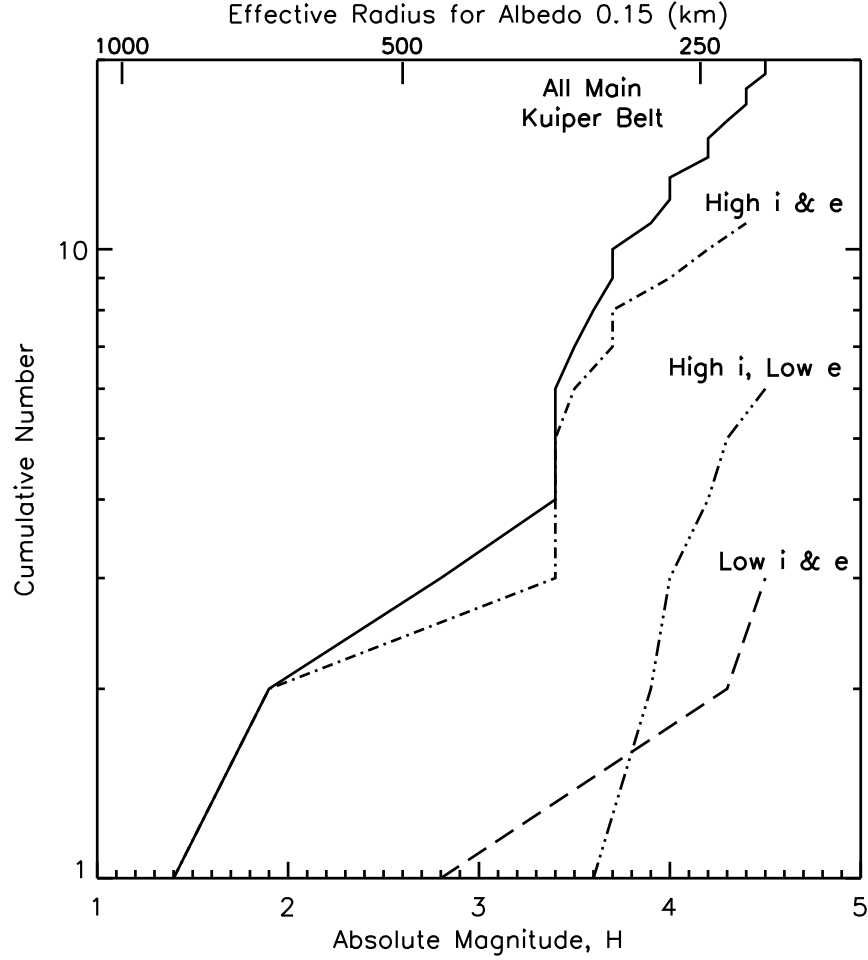
Fig. 12.— The absolute magnitude versus the cumulative number of objects in the main Kuiper Belt (solid line) and its subcategories. The largest few objects have had their absolute magnitudes adjusted as in Figure 8 to account for their higher albedos compared to the smaller objects. The high inclination ($i > 10$ degrees) and eccentricity ($e > 0.13$) objects (dotted dashed line) dominate the main Kuiper Belt on the large end. There appears to be a sizable group of main Kuiper Belt objects that have high inclinations but low eccentricities ($e < 0.07$) (triple dotted dashed line). These high i and low e objects could be related to either of the other subcategories in this figure. Large low inclination and low eccentricity objects (long dashed line) are very rare with only Quaoar being brighter than an absolute magnitude of 4.2.